Iron-Histidine Resonance Raman Band of Deoxyheme Proteins: Effects of Anharmonic Coupling and Glass-Liquid Phase Transition

Arkady Bitler* and Solomon S. Stavrov#

Department of Physiology and Pharmacology,* and Sackler Institute of Molecular Medicine, Department of Human Genetics and Molecular Medicine,# Sackler Faculty of Medicine, Tel Aviv University, Ramat Aviv, Tel Aviv 69978, Israel

ABSTRACT Weak anharmonic coupling of two soft molecular vibrations is shown to cause pronounced temperature dependence of the corresponding resonance Raman bands. The developed theory is used to interpret the temperature dependence of the iron-histidine band of deoxyheme proteins and model compounds. It is shown that anharmonic coupling of the iron-histidine and heme doming vibrations must cause pronounced broadening of the band, its asymmetry, and shift of its maximum to the red upon heating. It also can lead to a structured shape of this band at room temperature. Proper consideration of the anharmonic coupling allows simulation of the temperature dependence of the iron-histidine band shape of horse heart myoglobin in the temperature interval of 10–300 K, using the minimum number of necessary parameters. Analysis of this temperature dependence clearly shows that the iron-histidine band of deoxyheme proteins is sensitive to the glass-liquid phase transition in the protein hydration shell, which takes place at 160–190 K.

INTRODUCTION

A central problem of modern protein chemistry and physics is that of a mechanism of the effect of protein globule structure and dynamics on the structure and functioning of the protein active center. Heme proteins contain iron-porphyrin, Fe(P), as an isolated active center (see Fig. 1), which can be probed by a variety of spectroscopic techniques that provide information about protein-heme interactions. In hemoglobin (Hb), myoglobin (Mb), and some other heme proteins a bond between the iron and imidazole (Im) nitrogen of proximal histidine (Fe-N_{Im}) is the only covalent bond between the heme and the protein (for a review, see Perutz, 1989). Therefore, any experimental technique that allows the direct study of this bond is very useful for an elucidation of the interaction under consideration.

Nagai and Kitagawa (1980), Hori and Kitagawa (1980), and Kitagawa (1988) showed that resonance Raman scattering spectra of Fe(P)(Im) complexes and deoxyheme proteins (HPs) contain a band in the region of 200–250 cm^{-1}. They assigned this band to the scattering by the Fe-N_{Im} vibration. The position and intensity of this band essentially depend on the protein nature and conformation and on the type of environment (Sage et al., 1995; Kitagawa, 1988; Rousseau and Friedman, 1988; Spiro, 1988; Egeberg et al., 1990; Bosenbeck et al., 1992; Zhu et al., 1993; Hirota et al., 1996; Christian et al., 1997). This band was widely used to study the structure and, in combination with the flash photolysis technique, the dynamics of HPs (Rousseau and Friedman, 1988).

A number of studies revealed the substantial temperature dependence of this band, both in proteins (Ondrias et al., 1983; Sassaroli et al., 1986; Rousseau and Friedman, 1988; Ahmed et al., 1991; Gilch et al., 1993, 1995, 1996) and in Fe(P)(Im) complexes (Chaudhury et al., 1992); the band shifts to lower frequencies and broadens upon heating.

Two mechanisms were proposed to interpret this temperature dependence. The first one (Gilch et al., 1993, 1995, 1996) invokes an idea of temperature-dependent equilibrium of several specific protein conformational substates (CSs) (Frauenfelder et al., 1988). From this point of view temperature change affects a distribution of the system over CSs with different individual scattering properties, causing thermal broadening of the band and shift of its maximum.

Another approach (Ondrias et al., 1981, 1982b) considered the temperature dependence to be caused by anharmonic coupling of the Fe-N_{Im} vibration with another lower-frequency mode of the heme-imidazole unit. However, this interpretation was based on a theory (Shelby et al., 1979; Marks et al., 1980) developed for the case of a rigid vibration (the vibrational quantum is much greater than the temperature of the experiment) that interacts with a soft vibration. In the case under consideration, the opposite situation takes place: the Fe-N_{Im} vibrational quantum is approximately equal to thermal energy at room temperature. Consequently, the effect of the population of excited Fe-N_{Im} vibrational states on the corresponding resonance Raman band must be taken into account.

It was shown recently (Stavrov, 1993; Stavrov and Kushkuley, 1993) that in HPs and their models a change in the iron displacement out of a plane of the four porphyrin nitrogens (R) changes the frequency of the Fe-N_{Im} vibration. In other words, there is an anharmonic interaction between the Fe-N_{Im} vibration and a vibration of the iron together with the imidazole with respect to the porphyrin ring, Fe-P vibration.

Received for publication 21 December 1998 and in final form 23 July 1999.

Address reprint requests to Dr. Solomon S. Stavrov, Department of Human Genetics and Molecular Medicine, Sackler Faculty of Medicine, Tel Aviv University, Ramat Aviv, P.O. Box 39040, Tel Aviv 69978, Israel. Tel.: 972-3-640-9859; Fax: 972-3-640-5168; E-mail: stavrov@post.tau.ac.il.

0006-3495/99/11/2764/13 $2.00

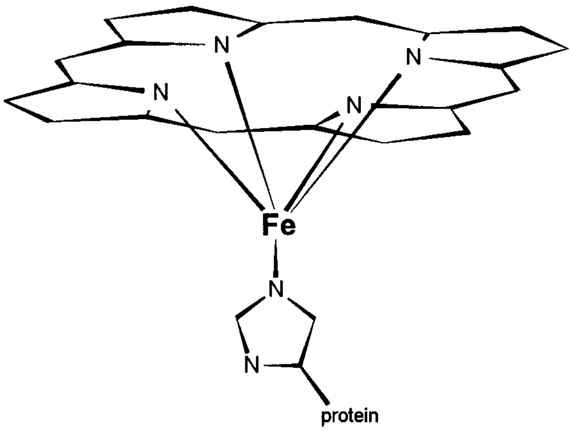

FIGURE 1 Schematic representation of the heme-histidine unit of deoxyheme proteins.

In this work, a brief review of the previously developed theoretical description of a weak anharmonic interaction between two soft vibrations (Rosenfeld and Stavrov, 1994) will be presented. Its effect on a shape of the corresponding resonance Raman band will be studied. The results will be used to interpret a shape of the Fe-N_{Im} resonance Raman band of different HPs and, in particular, horse heart myoglobin (hhMb).

METHODS

Method of moments

Zero (M_0), first (M_1), and second (M_2) moments of a band $F(\omega)$ are defined as (Lax, 1952; Markham, 1959)

$$M_0 = \int_0^\infty F(\omega)\mathrm{d}\omega$$

$$M_1 = \int_0^\infty F(\omega)\omega\,\mathrm{d}\omega/M_0 \tag{1}$$

$$M_2 = \int_0^\infty F(\omega)\omega^2\mathrm{d}\omega/M_0 - M_1^2.$$

These moments provide information on the intensity, center of gravity, and width of the band, respectively. In the case of a Gaussian band M_1 gives the band's maximum position, and M_2 is proportional to the square of the band's full width at half-maximum (FWHM).

Data processing

To provide a reliable and automated data analysis, we developed an original program package based on MATLAB 5.2. The fitting procedure was carried out using constrained nonlinear optimization method. The optimization program uses a sequential quadratic programming method based on quadratic approximation and minimization of the Lagrangian function. The optimization was carried out in the sense of least squares.

The quality and the statistical significance of the fit were judged by reduced χ_R^2 numbers:

$$\chi_R^2 = \sum_{i=1}^{N} \frac{(I_{i,\exp} - I_{i,\mathrm{fit}})^2}{\sigma_i^2 \cdot (N_0 - k_0 + 1)}, \tag{2}$$

where $I_{\exp}$ and I_{fit} are corresponding experimental and theoretical intensities, N_0 is the number of data points in each spectrum, σ_i denotes statistical errors of $I_{i,\exp}$, and k_0 is the number of free parameters in the fit. Acceptable and statistically significant fitting requires (Bevington, 1969)

$$1 < \chi_R^2 < 2. \tag{3}$$

The statistical errors were used instead of standard deviations because only one experimental spectrum for each temperature was available to us. σ_i were calculated from the experimental data by a sliding window method, and the linear trend was subtracted from data sample for each window position:

$$\sigma_i = \sqrt{\frac{\sum_{j=i-\theta}^{i+\theta} (\mathrm{detr}(I_{i,\exp}))^2 - \frac{\left(\sum_{j=i-\theta}^{j=i+\theta} \mathrm{detr}(I_{i,\exp})\right)^2}{N_0}}{N_0 - 1}}. \tag{4}$$

To obtain a magnitude of θ, each spectrum was fitted by three Gaussians, and the corresponding χ_R^2 values were calculated using Eq. 4. Then they were compared to those obtained using standard deviations (see Table 1 by Gilch et al., 1995). The best agreement was achieved at $\theta = 15$; this magnitude was used in the following data processing.

EFFECT OF THE ANHARMONIC INTERACTION ON THE STRUCTURE AND ENERGY SPECTRUM OF THE SYSTEM

The basic description of the problem is given in terms of a zero-order Hamiltonian (H_0), which describes energy levels of independent Fe-P and Fe-N_{Im} oscillators with vibrational quanta $\hbar\Omega_0$ and $\hbar\omega_0$ ($\Omega_0 > \omega_0$) and an interaction H_{anh} that couples these modes:

$$H = H_0 + H_{\mathrm{anh}},$$

$$H_0 = \frac{\mathbf{P}^2}{2M} + \frac{\mathbf{p}^2}{2m} + \frac{1}{2}M\Omega_0^2\,\mathrm{Q}^2 + \frac{1}{2}m\omega_0^2\,q^2, \tag{5}$$

$$H_{\mathrm{anh}} = \frac{1}{2}M\Omega_0^2\,\mathrm{Q}^2(\beta q^2 + 2\alpha q),$$

where $\mathbf{P}$ and $\mathbf{p}$, M and m, and Q and q are moments, masses, and initial displacements from equilibrium positions of the Fe-P and Fe-N_{Im} modes, respectively, and α and β are constants of the linear and quadratic anharmonic coupling, respectively.

Using second-order perturbation theory, taking into account only terms linear and quadratic in q, and neglecting terms proportional to $(\omega_0/\Omega_0)^2 \ll 1$, Rosenfeld and Stavrov (1994) obtained the following expression for eigenvalues of the Hamiltonian in Eq. 5:

$$E_{\mathrm{N,n}} = \hbar\Omega_0\left(N + \frac{1}{2}\right) + \hbar\omega_0\left(n + \frac{1}{2}\right) - \frac{\xi}{2}\hbar\Omega_0\left(N + \frac{1}{2}\right)^2\left[1 + 2\gamma\frac{\left(n + \frac{1}{2}\right)}{\left(N + \frac{1}{2}\right)}\right], \qquad (6)$$

where

$$\gamma = \frac{\omega_0}{2\Omega_0}\left(1 - \frac{\beta}{\alpha^2}\right); \qquad (7)$$

N and n are population numbers of the Fe-P and Fe-$\mathrm{N_{Im}}$ modes, respectively, and

$$\xi = \frac{\hbar\Omega_0\alpha^2}{m\omega_0^2} \qquad (8)$$

is a dimensionless parameter of the linear anharmonicity.

Using eigenfunctions of the Hamiltonian in Eq. 5, Rosenfeld and Stavrov (1994) showed that an equilibrium coordinate of the Fe-P oscillator is differently affected by the anharmonic coupling in different states of the Fe-$\mathrm{N_{Im}}$ subsystem: the greater N is, the greater is its displacement $q_{0,\mathrm{N}}$:

$$q_{0,\mathrm{N}} = -\frac{\xi}{\alpha}\left(N + \frac{1}{2}\right) \qquad (9)$$

A cross section of energy surfaces of the whole Fe(P)(Im) system along the q coordinate is schematically presented in Fig. 2. It follows from this scheme that population of the Fe-$\mathrm{N_{Im}}$ excited states upon heating causes the appearance of additional scattering bands of lower frequency. In the next section, the effect of these bands on the shape and position of the whole Fe-$\mathrm{N_{Im}}$ band will be studied.

A magnitude of the thermal R change (q_0) can be calculated by

$$q_0 = \langle q_{0,\mathrm{N}} - q_{0,0}\rangle_{\mathrm{T}}, \qquad (10)$$

where $\langle(\ldots)\rangle_{\mathrm{T}}$ is understood to be a sum of the $(\ldots)$ values over all initial states of a system multiplied by the thermal population of each of them:

$$\langle(\ldots)\rangle_{\mathrm{T}} = \left[\sum_{\mathrm{N,n}}\exp\left(-\frac{E_{\mathrm{N,n}}}{kT}\right)(\ldots)\right]\left[\sum_{\mathrm{N,n}}\exp\left(-\frac{E_{\mathrm{N,n}}}{kT}\right)\right]^{-1}, \qquad (11)$$

and k is Boltzmann's constant.

Rosenfeld and Stavrov (1994) obtained anharmonic corrections to $E_{\mathrm{N,n}}$ that are proportional to ξ, the higher degrees of this parameter not contributing into $E_{\mathrm{N,n}}$ in the frameworks of second-order perturbation theory (see Eq. 6). The same accuracy must be kept in Eq. 11.

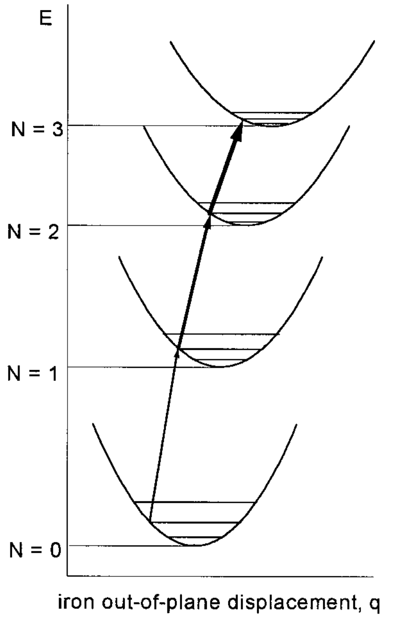

FIGURE 2 Schematic representation of a cross section of adiabatic potential surfaces of the Fe(P)(Im) complex in the direction of the iron displacement out of the porphyrin plane. The arrows describe the transitions of the system due to the resonance Raman scattering by the Nth state of the Fe-$\mathrm{N_{Im}}$ subsystem: the larger N is, the stronger is the scattering (see Eq. 18).

Expanding the exponents in powers of ξ, keeping only terms linear in ξ, and taking advantage of relationships

$$\begin{aligned}\langle N\rangle_0 &= \frac{1}{2}\left[\coth\left(\frac{\hbar\Omega_0}{2kT}\right) - 1\right]\\ \langle N^2\rangle_0 &= \langle N\rangle_0 + 2\langle N\rangle_0^2 \qquad (12)\\ \langle N^3\rangle_0 &= \langle N\rangle_0 + 6\langle N\rangle_0^2 + 6\langle N\rangle_0^3,\end{aligned}$$

one obtains

$$\begin{aligned}\langle(\ldots)\rangle_{\mathrm{T}} &= \left\langle\left\{1 + \xi\frac{\hbar\Omega_0}{2kT}(N + ½)[N + ½ - \gamma(2n + 1)]\right\}(\ldots)\right\rangle_0\\ &\quad * \left\{1 - \xi\frac{\hbar\Omega_0}{4kT}\left[\coth^2\left(\frac{\hbar\Omega_0}{2kT}\right) - ½ - \gamma\coth\left(\frac{\hbar\Omega_0}{2kT}\right)\coth\left(\frac{\hbar\omega_0}{2kT}\right)\right]\right\}, \qquad (13)\end{aligned}$$

where

$$\langle(\ldots)\rangle_0 = \left[\sum_{\mathrm{N,n}}\exp\left(-\frac{N\hbar\Omega_0 + n\hbar\omega_0}{kT}\right)(\ldots)\right] \cdot\left[\cdot\sum_{\mathrm{N,n}}\exp\left(-\frac{N\hbar\Omega_0 + n\hbar\omega_0}{kT}\right)\right]^{-1}. \qquad (14)$$

Relationships 9, 10, 12, and 13 allow us to calculate q_0:

$$q_0 = -\frac{\xi}{2\alpha}\left[\coth\left(\frac{\hbar\Omega_0}{2kT}\right) - 1\right]. \tag{15}$$

Parameters contributing to Eqs. 5–15 can be estimated from a number of experiments: $\hbar\Omega_0 \approx 225\ \mathrm{cm}^{-1}$ (Gilch et al., 1993, 1995); $\hbar\omega_0 \approx 50-80\ \mathrm{cm}^{-1}$ and $m\omega_0^2 \approx 9600\ \mathrm{cm}^{-1}$ $\mathrm{Å}^{-2}$ (Parak et al., 1982; Šrajer and Champion, 1991; Champion, 1992; Li and Zgierski, 1992). α and ξ can be estimated from a correlation (Stavrov, 1993) between changes in the maximum position of the Fe-$\mathrm{N_{Im}}$ band ($\Omega_{\max}$) and R (measured in Å) in different Fe(P)(Im) complexes,

$$\Delta\Omega_{\max}/\Omega_{\max} \approx -0.9\Delta R, \tag{16}$$

the relationship between the small changes in the force-field constant and frequency,

$$\Delta K = M(\Omega_{\max} + \Delta\Omega_{\max})^2 - M\Omega_{\max}^2 \approx 2M\Omega_{\max}^2\frac{\Delta\Omega_{\max}}{\Omega_{\max}}, \tag{17}$$

and the Hamiltonian in Eq. 5, $\alpha \approx -0.9\ \mathrm{Å}^{-1}$ and $\xi \approx 0.02$. Quadratic anharmonic coupling is also assumed to be weak, $-2\ \mathrm{Å}^{-1} \leq \beta \leq 2\ \mathrm{Å}^{-1}$ (Rosenfeld and Stavrov, 1994).

Taking advantage of these values, one obtains that at room temperature R is larger by ~0.01 Å than at cryogenic temperatures.

The results obtained in this section also allow us to explain some peculiarities of the relaxation of the cryogenic product (Mb*) of Mb(CO) photolysis. It is well known that at cryogenic temperatures any change in the protein structure is hindered by the glassy environment. Therefore, Mb* is observed in some nonrelaxed protein conformations. For example, Sassaroli et al. (1986), Rousseau and Argade (1986), Powers et al. (1987), Rousseau and Friedman (1988), Ahmed et al. (1991), Steinbach et al. (1991), Nienhaus et al. (1992b), and Sage et al. (1995) showed that the Fe-$\mathrm{N_{Im}}$ RR band and optical absorption band III of Mb* are located at higher and lower energies, respectively, than those of Mb at the same temperatures. This difference manifests a smaller R in Mb* than in Mb (Stavrov, 1993); this conclusion is supported by the latest cryogenic x-ray diffraction studies of Mb* (Hartmann et al., 1996; Schlichting et al., 1994; Teng et al., 1994, 1997). Because R in Mb is mainly controlled by interactions in the heme-imidazole unit (Gelin et al., 1983), the experimental results presented above imply that at cryogenic temperatures the protein does not allow full intrinsic heme relaxation.

However, Nienhaus et al. (1994), Abadan et al. (1995), and Chu et al. (1995) showed recently that illumination of Mb* imbedded in a glassy matrix causes its relaxation toward the deoxy structure. This light-induced relaxation (LIR) can be qualitatively explained in the frameworks of the developed theory.

Henry et al. (1986) showed, using molecular dynamics simulations and assuming Boltzmann distribution of the excitation energy over all heme vibrations, that an absorption of a 530- or 353-nm photon by the heme increases its temperature by 500–700 K. The conclusion about strong heme heating upon illumination was also supported by the experimentally observed residual overheat of Hb (Petrich et al., 1987; Lingle et al., 1991; Simpson et al., 1997). Therefore, the 513- and 488-nm illumination (Nienhaus et al., 1994; Abadan et al., 1995; Chu et al., 1995) is expected to increase the heme vibrational temperature by ~600 K. It follows from Eq. 15 that such heating must increase R by ~0.03 Å, implying that an absorption of each photon causes a sudden increase in R. Because in Mb* R is smaller than its equilibrium value and because the heme is surrounded by glassy media, it is reasonable to assume that some residual protein deformation persists after the heme vibrational temperature decay. Consequently, each act of photon absorption leads to some protein relaxation toward its deoxy conformation. Because during the LIR experiment ~10^5 photons are absorbed by each heme, even very small residual protein deformations persisting after each photon absorption can lead to considerable cumulative protein relaxation toward the deoxy conformation. It is clear that the effect of the illumination must depend on the number of photons absorbed and not on the light intensity or duration separately; this conclusion is in full agreement with experiments by Nienhaus et al. (1994), Abadan et al. (1995), and Chu et al. (1995).

Note that the Boltzmann distribution of the excitation energy was assumed only to estimate the sudden R increase and is not necessary for this increase. Indeed, Stavrov (1993) showed that in the heme B and Q excited electronic states the Fe-$\mathrm{N_{Im}}$ bond is considerably shorter than in the ground electronic state. Consequently, a decay of the B or Q excited electronic state to the ground state must essentially populate the Fe-$\mathrm{N_{Im}}$ excited vibrational states, which are characterized by the considerably larger R displacement (see Eq. 9).

The R enlargement increases the effective barrier to CO rebinding (Jortner and Ulstrup, 1979; Agmon and Hopfield, 1983; Buhks and Jortner, 1985; Šrajer et al., 1988; Liddington et al., 1988); this increase is observed experimentally in the LIR experiments (Nienhaus et al., 1994; Abadan et al., 1995; Chu et al., 1995).

EFFECT OF ANHARMONIC COUPLING ON THE TEMPERATURE DEPENDENCE OF THE RESONANCE RAMAN Fe-$\mathrm{N_{Im}}$ BAND

We assume that the excitation energy satisfies two criteria: 1) it is close enough to the energy of an excited electronic state to take into account an interaction with this state only, and 2) it is far enough from a resonance with the vibrational satellites to allow averaging of the scattering probability over vibrational states. In this case, an intensity of each RR band corresponding to the N, $n \rightarrow N + 1$, n scattering is proportional to

$$|\langle N+1|Q|N\rangle|^2 \sim 1 + N \tag{18}$$

and to a square of the first derivative of the polarization tensor, $\alpha_{00}(q_{0,\mathrm{N}})$ (Koningstein, 1972). Describing a shape of each N, $n \rightarrow N + 1$, n scattering band by $F_0(\omega - \Delta E_{\mathrm{N,n}})$, one obtains the following expression for this band:

$$F_{\mathrm{N,n}}(\omega) \sim \left| \left[\frac{\partial \alpha_{00}(q_{0,\mathrm{N}})}{\partial Q} \right]_{\mathrm{Q}=0} \right|^2 (1 + N) F_0(\omega - \Delta E_{\mathrm{N,n}}), \quad (19)$$

where $\Delta E_{\mathrm{N,n}}$ is an energy gap between two closest Fe-$\mathrm{N_{Im}}$ states (Eq. 6):

$$\Delta E_{\mathrm{N,n}} = E_{\mathrm{N+1,n}} - E_{\mathrm{N,n}} = \Omega_0\{1 - \xi[1 + N + \gamma(n + \tfrac{1}{2})]\}. \quad (20)$$

Neglecting for simplicity the dependence of $\alpha_{00}(q_{0,\mathrm{N}})$ on N (see Eq. 19), keeping only temperature-dependent terms and using the abbreviation in Eq. 11, the following expression for the shape of the band formed by all of the N, $n \rightarrow N + 1$, n transitions can be obtained:

$$F(\omega) = \langle (1 + N) F_0(\omega - \Delta E_{\mathrm{N,n}}) \rangle_{\mathrm{T}}. \quad (21)$$

It follows from Eq. 21 that the thermal population of excited vibrational states leads to the formation of a band, the width and position of which depend on the temperature. The situation is presented schematically in Fig. 2. To analyze this temperature dependence analytically, the first three moments of the band (see Eq. 1) are calculated.

Using the relationships in Eqs. 12–14 and analogous formulae for $\langle n \rangle_{\mathrm{T}}$ and neglecting terms proportional to $(\omega_0/\Omega_0)^2$ and the width of each contribution, one obtains from Eqs. 1, 20, and 21

$$\begin{aligned} M_0 &= \frac{1}{2}\left[\coth\left(\frac{\hbar\Omega}{2kT}\right) + 1\right]\left\{1 + \xi\frac{\hbar\Omega}{2kT}\left[\coth\left(\frac{\hbar\Omega}{2kT}\right) - 1\right]\right. \\ &\qquad \cdot\left[\coth\left(\frac{\hbar\Omega}{2kT}\right) - 1 - \frac{1}{2}\gamma\left[\coth\left(\frac{\hbar\omega_0}{2kT}\right) + 1\right]\right], \\ M_1 &= \Omega\left\{1 - \xi\left[\coth\left(\frac{\hbar\Omega}{2kT}\right) - 1 + \frac{1}{2}\gamma\left[\coth\left(\frac{\hbar\omega_0}{2kT}\right) - 1\right]\right]\right\}, \\ M_2 &= \frac{1}{2}\Omega^2\xi^2\left\{\coth^2\left(\frac{\hbar\Omega}{2kT}\right) - 1 + \frac{1}{2}\gamma^2\left[\coth^2\left(\frac{\hbar\omega_0}{2kT}\right) - 1\right]\right\}, \end{aligned} \quad (22)$$

where

$$\Omega = \Omega_0[1 - \xi(1 + \tfrac{1}{2}\gamma)] \quad (23)$$

is a frequency of the light scattered at zero temperature (see Eq. 20).

In Eq. 22 the terms $\coth(\hbar\Omega_0/2kT) - 1$ and $\coth^2(\hbar\Omega_0/2kT) - 1$ describe the effect of the Fe-$\mathrm{N_{Im}}$ excited state population and weakly depend on the temperature at low temperatures ($T < ½\hbar\Omega_0$). The terms proportional to $\coth(\hbar\omega_0/2kT) - 1$ and $\coth^2(\hbar\omega_0/2kT) - 1$ stem from a contribution of the Fe-P excited states. It can be shown using magnitudes of the parameters (see the end of the previous section) that these terms are also small in the temperature interval under consideration. Therefore at low temperatures the band shape is expected to change weakly.

At higher temperatures, $T \geq ½\hbar\Omega_0$, the Fe-$\mathrm{N_{Im}}$ excited states become notably occupied. Their contributions to the light scattering lead to the essential temperature dependence of all three moments.

The temperature dependence of the Fe-$\mathrm{N_{Im}}$ band shape can be simulated using Eq. 21 and the magnitudes of the parameters presented in this section and, for the sake of simplicity, neglecting the previous contribution from the terms proportional to γ. Results of the calculation are presented in Fig. 3. They show that the band shape hardly depends on temperature at $T < 100$ K and becomes strongly temperature dependent at $T > 150$ K; this conclusion is in full agreement with the results of the method of moments. Fig. 4 shows that at room temperature the band shape strongly depends on the strength of the anharmonic coupling. Its strengthening increases separation between the individual N, $n \rightarrow N + 1$, n bands, making them observable. Obviously, the smaller the width of the individual contribution, the smaller ξ must be to make the band structured.

The latter conclusion can be used to give an alternative explanation for the following experimental observation. La Mar et al. (1977), Nagai and Kitagawa (1980), Nagai et al. (1982), Ondrias et al. (1982a), Kitagawa (1988), and Rousseau and Friedman (1988) showed that at room temperature both β subunits of Hb are characterized by their own isotropic chemical shift ($\delta(\beta)$), frequency of the porphyrin breathing mode ($\nu_4(\beta)$), and Fe-$\mathrm{N_{Im}}$ frequency ($\Omega(\beta)$) values. The α chains show other $\delta(\alpha)$ and $\nu_4(\alpha)$ values, whereas the Fe-$\mathrm{N_{Im}}(\alpha)$ band consists of two peaks separated by $\sim$10 $\mathrm{cm^{-1}}$. Ondrias et al. (1982a) assigned these peaks to two CSs. Note that the latter interpretation cannot explain why these CSs are characterized by the same $\nu_4(\alpha)$ value. This is especially strange because the 16 $\mathrm{cm^{-1}}$ increase in $\Omega(\alpha)$ upon the T → R transition is accompanied by a 2.4 $\mathrm{cm^{-1}}$ decrease in $\nu_4(\alpha)$ (Ondrias et al., 1982a); this result shows that $\nu_4(\alpha)$ is sensitive to the protein conformational changes. At the same time two peaks of the Fe-$\mathrm{N_{Im}}(\alpha)$ band can easily be explained as a manifestation of the anharmonic coupling (see Fig. 4), which is stronger in the α chain than in the β chain. Indeed, such an anharmonic coupling can split the band of the α chain and only broaden that of the β chain; this interpretation naturally explains the single value of $\nu_4(\alpha)$. Moreover, it follows from this interpretation that the sample cooling should 1) eliminate the Fe-$\mathrm{N_{Im}}(\alpha)$ band splitting, 2) strongly reduce the difference between $\Omega(\alpha)$ and $\Omega(\beta)$, and 3) increase both $\Omega(\alpha)$ and $\Omega(\beta)$. All of these conclusions are in full agreement with the experimental data (Ondrias et al., 1982a, 1983).

TEMPERATURE DEPENDENCE OF THE Fe-$\mathrm{N_{Im}}$ RESONANCE RAMAN BAND OF HORSE HEART MYOGLOBIN

Gilch et al. (1993, 1995) studied experimentally the temperature dependence of the RR spectrum of hhMb in the

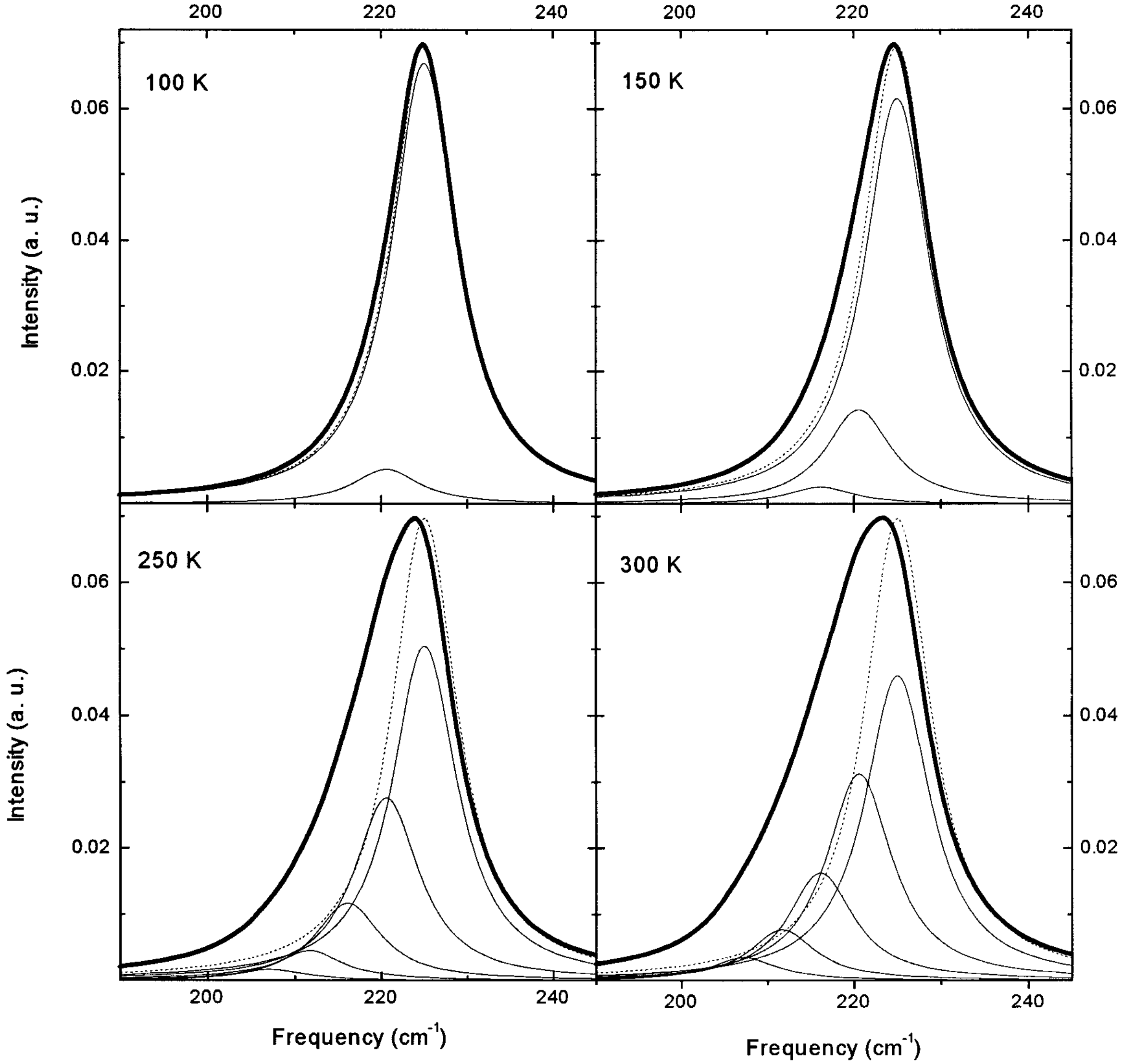

FIGURE 3 Shape of the Fe-N$_{\rm Im}$ resonance Raman band (*thick curve*) at different temperatures compared to that at zero temperature (*dashed curve*) and individual contributions of the *N*th states (*thin curves*). The individual contributions from the states with $N \leq 4$ and $n \leq 8$ are taken into account and are simulated by Lorentzians with FWHM = 9 cm^{-1}.

frequency interval of 160–260 cm^{-1} (Fig. 5, *open squares*). This interval contains three overlapped bands, the central one of which is assigned to Fe-N$_{\rm Im}$. The higher-energy one (band 2) most probably corresponds to the scattering by a pyrrole rocking vibration (Rousseau and Friedman, 1988), whereas the origin of the lower-energy band (band 1) is still unclear. In this section the developed theory is used to interpret the temperature dependence under consideration.

We assume that width of each band makes considerable inhomogeneous contributions, and therefore bands 1 and 2 and each component of band 3 are described by Gaussians (their FWHMs are defined below on as Γ_1, Γ_2, and Γ, respectively). In this case, the fitting function has the form

$$I_{\rm fit} = \frac{1}{2}\sum_{\rm i=1}^{2} I_{\rm i}\left[1 + \coth\left(\frac{\hbar\Omega_{\rm i}}{kT}\right)\right]F_{\rm i}(\omega - \Omega_{\rm i}) + IF(\omega), \qquad (24)$$

where the first sum describes the contributions of bands 1 and 2, and the last term corresponds to the Fe-N$_{\rm Im}$ band (Eq. 21). In this expression $I_{\rm i}$ and I are the relative intensities of these bands at zero temperature ($I_1 + I_2 + I = 1$), and $\Omega_{\rm i}$ are frequencies of vibrations corresponding to bands 1 and 2. In Eq. 24 we take into account the temperature dependence of intensities of bands 1 and 2 (Koningstein, 1972), and $F(\omega)$ is calculated considering the contribution from the states with $N \leq 4$ and $n \leq 8$.

Note that in the case of individual Gaussian bands the expressions in Eq. 22 for M_0 and M_1 still apply, whereas the second moment of the full band equals

$$M_2^{\rm G} = \frac{\Gamma^2}{8\log 2} + M_2. \qquad (25)$$

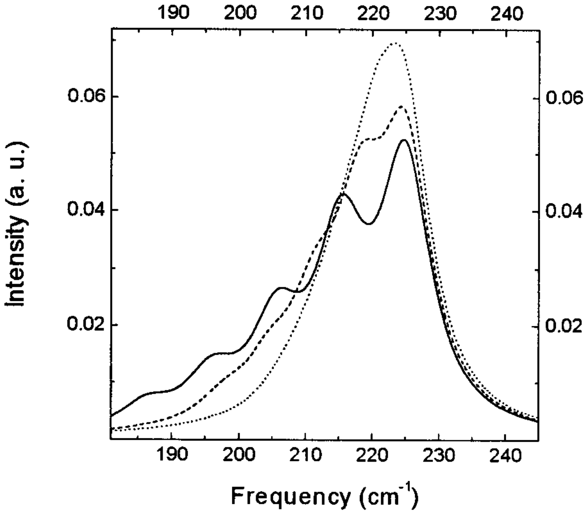

FIGURE 4 Dependence of a shape of the room temperature (300 K) Fe-N$_{\mathrm{Im}}$ resonance Raman band on α: -0.9 Å^{-1} (·····), -1.1 Å^{-1} (- - - - -), and -1.3 Å^{-1} (——).

To reduce the number of fitting parameters we neglect the terms of Eq. 6 that are proportional to γ. This reduces the number of terms controlling the temperature dependence of the Fe-N$_{\mathrm{Im}}$ band to one, ξ. Therefore, the fitting function (Eq. 24) contains nine independent parameters; this number is the minimum number of parameters that must be used to describe any temperature dependence of a normalized three-band spectrum.

Results

At the first stage, we assumed that the glass-liquid phase transition, which occurred in the protein-solvent system, did not affect the spectrum under consideration. In this case all of the parameters were the same in the whole temperature interval of 10–300 K, and all six spectra (set I) had to be fitted simultaneously, using Eq. 24. One sees from Table 1 that three of six corresponding χ^2_{R} values do not satisfy the criterion in Eq. 3. Consequently, the fit quality is not acceptable, and the assumption is wrong.

At the second stage we recognized that the glass-liquid phase transition could affect all of the parameters, and their magnitudes could differ below and above the transition temperature, $T_{\mathrm{gl}} \approx 160$–$190$ K (Settles and Doster, 1996; Demmel et al., 1997; Diehl et al., 1997). Accordingly, the experimental data were separated into two sets: the first contained the spectra obtained at temperatures of 10, 100, and 150 K (set II), and the second the spectra obtained at 200, 250, and 300 K (set III). Then these two sets were fitted separately. This separation considerably improved the fit quality and made it acceptable (see Table 1).

Note, however, that the improvement of the fit quality could stem simply from the reduction of the number of the experimental data that were fitted simultaneously—three spectra in each of the sets instead of six in set I. To check this possibility, two other three-spectra sets were formed. Each of the sets contained spectra corresponding to temperatures below and above T_{gl}: 100, 150, and 200 K (set IV) and 150, 200, and 250 K (set V). The corresponding χ^2_{R} are presented in Table 1, from which it follows that none of these sets can be fitted successfully with I_{fit}. Consequently, the manner of separation in the sets is specific and reflects the effect of the phase transition on the spectrum under consideration.

It is also possible that the temperature dependence stems only from the effect of the phase transition, the effect of the anharmonic coupling being negligibly weak. To test this possibility we fitted sets II and III separately, assuming $\alpha = 0$. The results on the fit quality are presented in sets II$_0$ and III$_0$ of Table 1 and show that both fits are unreliable. Consequently, consideration of the anharmonic coupling is crucial for any successful fit.

Finally, we tried to reduce the number of parameters that were affected by the phase transition. First, we found that a successful fit could be achieved, assuming that only the Fe-N$_{\mathrm{Im}}$ band and band 1 were affected by the phase transition and the band 2 was unchanged. Then the parameters of the former two bands were examined. It was found that the experimental curves could be fitted, assuming that the intensities of these two bands and the magnitude of Ω were affected by the transition and the other parameters were the same below and above T_{gl}. The fit quality is worse in this case (see Table 1, set IIIa) but still acceptable. A graph of the successful fit and magnitudes of the parameters are presented in Fig. 4 (sets II and III, *thick solid line*) and in Table 2 (sets II, III and IIIa), respectively.

Discussion

It follows from Table 1 and Fig. 5 that the temperature dependence of the RR spectrum in the interval of 160–260 cm^{-1} can be explained, assuming that it is affected by both the glass-liquid phase transition and the anharmonic coupling between the Fe-N$_{\mathrm{Im}}$ and Fe-P vibrations.

The first assumption appears to be well founded because it is known that the glass-liquid phase transition in the protein hydration shell occurs at 160–190 K (Settles and Doster, 1996; Demmel et al., 1997; Diehl et al., 1997) and affects the results of all of the experimental techniques used: dynamics of carbon monoxide rebinding (Austin et al., 1975; Ansari et al., 1987; Steinbach et al., 1991; Post et al., 1993), x-ray diffraction (Frauenfelder et al., 1979; Hartmann et al., 1982; Parak and Knapp, 1984), Mössbauer spectroscopy (Dvivedi et al., 1979; Keller and Debrunner, 1980; Parak et al., 1982; Mayo et al., 1983; Parak and Knapp, 1984; Frauenfelder et al., 1988; Nienhaus et al., 1992a; Melchers et al., 1995), inelastic neutron (Doster et al., 1989; Cusack and Doster, 1990) and x-ray (Achterhold et al., 1996) scatterings, optical absorption spectroscopy in the visible and close ultraviolet intervals (Cordone et al., 1986, 1988; Di Iorio et al., 1991; Di Pace et al., 1992;

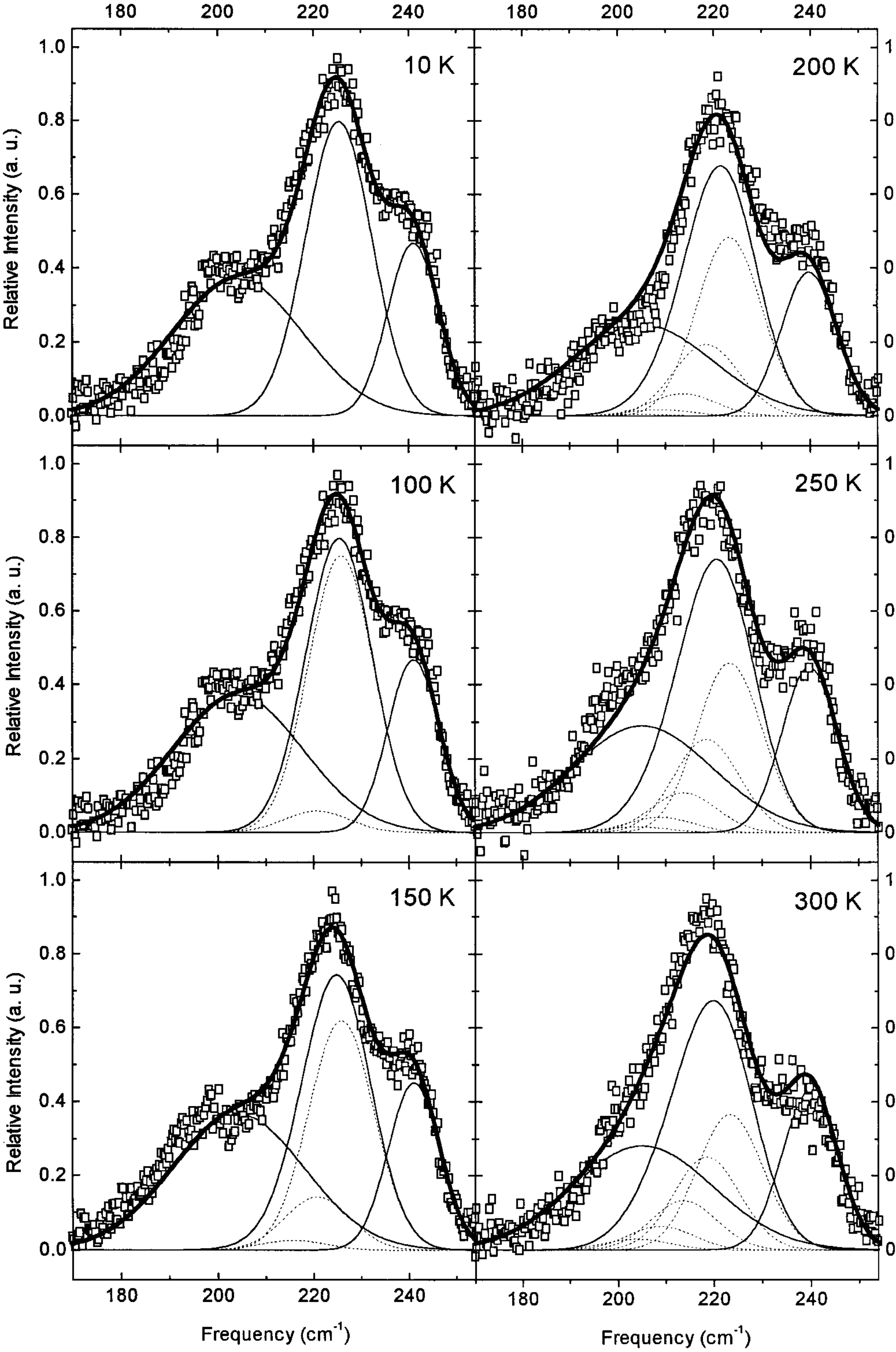

FIGURE 5 Spectra of resonance Raman scattering obtained at different temperatures: experimental data by Gilch et al. (1995) (*empty squares*), theoretical curve obtained using Eq. 24 (*thick solid curve*), curves corresponding to bands 1, Fe-N$_{\mathrm{Im}}$, and 3 (*thin solid curves*), and individual contributions to the Fe-N$_{\mathrm{Im}}$ band from *N*th vibrational states (*dashed curves*).

Nienhaus et al., 1992b; Cupane et al., 1993; Boffi et al., 1994), and pressure effects on infrared absorption (Frauenfelder et al., 1990) and resonance Raman (Galkin et al., 1997) spectra. Melchers et al. (1995) showed that changes in the optical absorption Soret band stem mainly from changes in the structure and/or dynamics of the heme group and its closest environment. All of these results show that the phase transition induces changes in the structure and

TABLE 1 χ_R^2 values characterizing the quality of different fits of the experimental data at different temperatures

Set number	10 K	100 K	150 K	200 K	250 K	300 K
I	2.1	1.5	2.9	2.4	1.5	2.2
II	1.8	1.3	1.9	—	—	—
III	—	—	—	1.5	1.4	1.4
IIIa	—	—	—	1.8	1.5	1.5
IV	—	1.5	2.1	2.2	—	—
V	—	—	2.5	2.1	1.4	—
II_0	2.3	1.3	2.4	—	—	—
III_0	—	—	—	3.2	1.5	1.9

dynamics of the whole protein and, in particular, in the electronic and vibrational structure of the heme-imidazole unit. Therefore some special reasons must be found to explain why such a sensitive technique like resonance Raman scattering should not reflect changes caused by this transition. It would be especially strange if the phase transition did not affect the Fe-N_{Im} band, which is coupled to the Soret band (Bangcharoenpaurpong et al., 1984), is the only chemical bond between the protein and the heme, and was shown to depend notably on the solvent nature (Sage et al., 1995) and the protein structure (see, for example, Rousseau and Friedman, 1988). Note that even visual inspection of the experimental spectra presented on Fig. 5 shows that the left-hand spectra ($T < T_{gl}$) qualitatively differ from the right-hand ones ($T > T_{gl}$): the former have a very pronounced shoulder and even a maximum in the lower-frequency part of the spectra, whereas in the latter this feature is much weaker. It follows from Fig. 5 and Table 2 that this characteristic spectral change is caused mainly by the change in the relative intensities of band 1 and the Fe-N_{Im} band: 0.9 at $T < T_{gl}$ and 0.4–0.6 at $T > T_{gl}$.

The second assumption is based on a conclusion (Stavrov, 1993) that the magnitude of the Fe-N_{Im} frequency is controlled by the heme doming, or, in other words, there is an anharmonic coupling between the Fe-P and Fe-N_{Im} vibrations (Rosenfeld and Stavrov, 1994). Note that ξ was obtained in the present paper in two ways: from a number of independent experiments (see end of the previous section) and from the above fitting procedure. The very close values (0.02 and 0.021 ÷ 0.022, respectively) obtained in both ways show that it is anharmonic coupling that controls the temperature dependence of the spectrum below and above T_{gl}.

The resonance Raman spectra under consideration are complicated; they consist of three overlapped bands. However, three facts ensure the reliability of our interpretation: 1) clear three band shapes of the experimental spectra at temperatures below T_{gl}; 2) successful simulation of the experimental spectra above and below T_{gl}, using only the minimum set of parameters; and 3) very close values of the anharmonic constant obtained from the fitting procedure and from a number of independent experiments. Therefore, although the complicated shape of the spectra can cause some uncertainty in the determination of the parameter magnitudes, this uncertainty cannot change the main conclusions of this paper.

The temperature dependence of the spectrum can be explained assuming that the phase transition affects only the intensities of band 1 and the Fe-N_{Im} band and the Ω magnitude (see Table 2). The considerable change in the intensities is caused by a change in the coupling of the corresponding vibrations with the Soret transition. This is not surprising because, as mentioned above, the position and shape of the Soret band are strongly affected by the glass-liquid phase transition. The weak change in Ω is caused by changes in the electronic structure of the heme-imidazole unit. These can be caused by alterations of the protein electric field due to changes in the protein structure and dynamics with the phase transition. This interpretation is supported by the fact that Ω is changed by $\sim$2 cm^{-1} with different replacements of distal imidazole that change the protein electric field on the heme (Hirota et al., 1996; Christian et al., 1997).

Note that the relatively large width of each $N, n \rightarrow N + 1, n$ subband ($\Gamma = 16$ cm^{-1}) justifies an assumption about the considerable contribution of inhomogeneous broadening to the Fe-N_{Im} band. This contribution can stem from a distribution of magnitudes of the heme doming in Mb molecules. However, this distribution is described by a Gaussian and does not assume some specific protein CSs.

The only parameter that appears to be out of the usual range is $\Gamma_1 \approx 32$–35 cm^{-1}; these values are considerably larger than FWHMs of other bands. Such a large magnitude can be due to different factors: strong sensitivity of this band to inhomogeneous protein distribution, contribution of the Rayleigh background, the possibility that it consists of a number of bands, etc. However, it is impossible to choose among these possibilities, because the nature of band 1 is not known.

Information about the relationship between contributions of the anharmonic coupling and phase transition to the temperature dependence of the Fe-N_{Im} band can be obtained from Fig. 6. It is seen from Fig. 6 *A* that temperature by itself weakly affects the relative intensity of this band with respect to band 2, $\sim$5%. The effect of the phase transition is much stronger, $\sim$15%. The center of gravity of the band, M_1, is shifted to the lower frequencies by both the anharmonic coupling and phase transition; the effect of the former is $\sim$2.5 times stronger than that of the latter, 5 and 2 cm^{-1}, respectively (Fig. 6 *B*). The width of the band is proportional to the square root of M_2. It is strongly affected by anharmonic coupling (at room temperature M_2 is about three times larger than that at zero temperature); the effect of the phase transition is negligibly weak (Fig. 6 *C*). It is also clear from Figs. 3 and 5 that at room temperature the Fe-N_{Im} band becomes strongly asymmetrical. Strong broadening and asymmetry of the Fe-N_{Im} band also contribute to the temperature shift of its maximum because of the overlap with band 1.

The discussion presented above clearly shows that RR spectra of hhMb in the frequency interval of 160–260 cm^{-1}

TABLE 2 Parameters of the bands contributing to the spectrum of the resonance Raman scattering

	I_1	Ω_1 (cm^{-1})	Γ_1 (cm^{-1})	I	Ω (cm^{-1})	Γ (cm^{-1})	ξ	I_2	Ω_2 (cm^{-1})	Γ_2 (cm^{-1})
$T < T_{gl}$ (set II)	0.38	204	32	0.42	226	16	0.022	0.20	241	13
$T > T_{gl}$ (set III)	0.24	202	32	0.54	223	16	0.020	0.22	240	13.5
$T > T_{gl}$ (set IIIa)	0.29	204	32	0.51	224	16	0.022	0.20	241	13

can be interpreted in the frameworks of already well-known and accepted mechanisms. On the contrary, the alternative model by Gilch et al. (1993, 1995, 1996) needs to postulate that 1) there are three specific CSs that are characterized by different Ω_0; 2) there is an intrinsic protein phase transition at $T_p \approx 110$ K; 3) this phase transition affects the protein distribution over the CSs under consideration and does not affect their thermodynamic and spectroscopic properties; and 4) the glass-liquid phase transition of the protein-solvent system at $T_{gl} \approx 160$–190 K affects neither the protein distribution over these CSs nor their thermodynamic and spectroscopic parameters. Note that it is very difficult to combine the last postulate with 1) the consequence of the same model (Gilch et al., 1996) that the solvent nature essentially affects entropy differences between these CSs and 2) essential changes in all of the studied optical absorption bands, including the Soret band, caused by this phase transition.

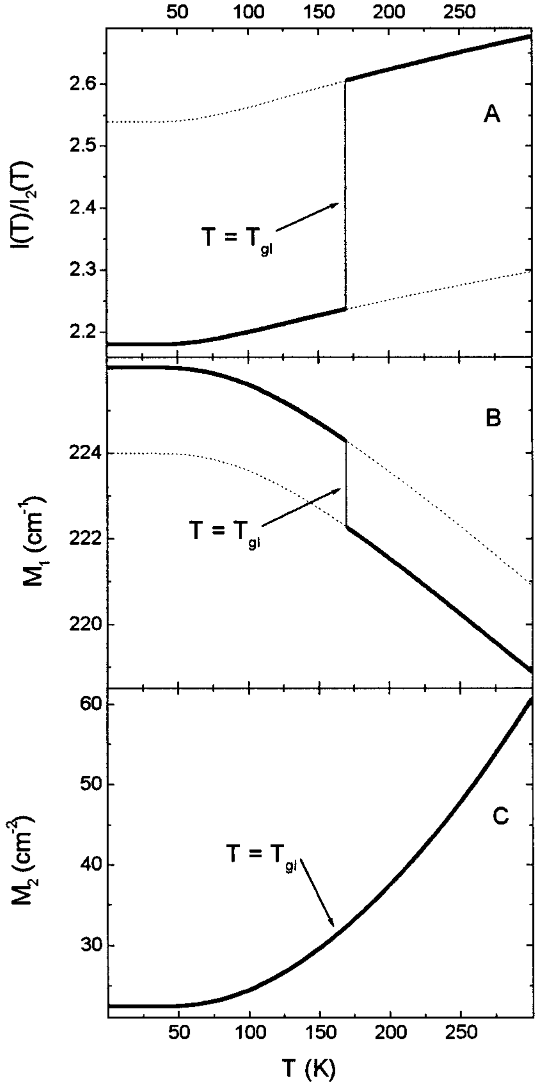

FIGURE 6 Temperature dependence of the relative intensity (*A*), and first (*B*) and second (*C*) moments of the Fe-N_{Im} resonance Raman band. The solid curves are obtained, taking into account the effect of the glass-liquid phase transition and anharmonic coupling, using Eqs. 22 and 25 and set IIIa of the parameters (see Table 2). The dashed curves are continuations of the corresponding curves into the temperature region of the other phase. For the sake of simplicity it is assumed that the phase transition occurs at 170 K and all of the parameters are changed stepwise.

Observation of the same basic features of the Fe-N_{Im} band of the model Fe(P)(Im) complex (Chaudhury et al., 1992) also supports our conclusion that the main contribution to the temperature dependence stems from the internal interactions in the heme-imidazole unit.

CONCLUSION

In this paper the influence of the anharmonic coupling between two low-frequency vibrations on the spectra of resonance Raman scattering was studied. The developed theory was used to study the general properties of the Fe-N_{Im} resonance Raman band of heme proteins and their models. It was shown that at $T \geq 150$ K the maximum position and width of the band depend on temperature, and the band becomes asymmetrical and can even become structured. These results explain qualitatively the experimentally observed temperature dependence of the Fe-N_{Im} resonance Raman band of different deoxyheme proteins and, in particular, the presence of two peaks in the hemoglobin α subunit at room temperature and the normal single peak band at cryogenic temperatures.

The strong broadening of the Fe-N_{Im} band at room temperature can also impede observation of the Fe-N_{Im} band in some heme proteins, even in the case of relatively strong coupling of the Fe-N_{Im} vibration with the corresponding optical transition (e.g., Soret band). If this is really the case, this band must appear at lower temperatures ($T \leq 100$ K).

The 10–300 K temperature dependence of the resonance Raman spectra of hhMb in the interval of 160–260 cm^{-1} was successfully fitted using the developed theory with the minimum number of necessary parameters. This result shows that both the anharmonic coupling under consideration and the glass-liquid phase transition of the solvent-protein system contribute to the temperature dependence; the contribution of the latter is weaker but still essential.

It was noted in the previous section that the experimental resonance Raman spectrum under consideration consists of three overlapped bands; this complicated shape could cause some uncertainty in the determination of the magnitudes of the parameters. To avoid the problem the Fe(P)(Im) model compounds can be tested because they 1) have a well-isolated Fe-N_{Im} resonance Raman band and 2) are not affected by the distribution of the protein over conformational substates. However, one must be careful because a change in the solvent phase state and temperature by itself can strongly affect the iron coordination number, the hydrogen bond between the imidazole and solvent molecules, etc. (see, for example, Wang and Brinigar, 1979). For example, Chaudhury et al. (1992) obtained spectra of Fe(PPDME)(2-MeIm) in dimethyl sulfoxide, the melting point of which equals 292 K (Windholz et al., 1976). This phase transition most probably affects the spectra and makes any quantitative interpretation questionable.

The conclusion about the influence of the glass-liquid phase transition on the resonance Raman spectra under consideration can be checked using solvents with different phase transition temperatures. First, the Soret band temperature dependence should be studied to find out if it is affected by the phase transition. If this is the case, the resonance Raman spectra should be obtained and fitted using T_{gl} obtained from the optical studies.

The developed theory allows interpretation of all of the experimental data in the framework of well known and accepted mechanisms. Obviously, this result cannot exclude the possibility that some specific conformational substates, if there are any, contribute to the overall shape of the Fe-N_{Im} band. However, it is clear that the experiment under discussion (Gilch et al., 1993, 1995) cannot be used to invoke an assumption about the presence of such specific conformational substates in deoxy hhMb. To our best knowledge there are no other experimental data supporting this assumption. Therefore, it appears to be superfluous.

Moreover, the very close magnitudes of the anharmonic coupling parameter were obtained in two independent ways: from the fitting procedure and from a number of other independent experiments. This result strongly supports our conclusion about the crucial contributions of both the anharmonic coupling and the glass-liquid phase transition to the temperature dependence of the Fe-N_{Im} resonance Raman band.

We thank Dr. Abel Schejter for helpful discussions and Dr. Reinhard Schweitzer-Stenner for providing us with results on the iron-histidine resonance Raman spectra before their publication and for helpful discussions.

This work was supported by the Sackler Fund for Scientists Absorption (SSS) and the Gileadi Program of the Center for Scientists Absorption, Ministry of Absorption of Israel.

Preliminary results were published by Rosenfeld and Stavrov (1994. *Chem. Phys. Lett.* 229:457–464).

REFERENCES

Abadan, Y., E. Y. T. Chien, K. Chu, C. D. Eng, G. U. Nienhaus, and S. G. Sligar. 1995. Ligand binding to heme proteins. V. Light-induced relaxation in proximal mutants L89I and H97F of carbonmonoxymyoglobin. *Biophys. J.* 68:2497–2504.

Achterhold, K., C. Keppler, U. van Bürk, W. Potzel, P. Schindelmann, E.-W. Knapp, B. Melchers, A. I. Chumakov, A. Q. R. Baron, R. Rüffer, and F. Parak. 1996. Temperature dependent inelastic x-ray scattering of synchrotron radiation of myoglobin analyzed by the Mössbauer effect. *Eur. Biophys. J.* 25:43–46.

Agmon, N., and J. J. Hopfield. 1983. CO binding to heme proteins: a model for barrier height distributions and slow conformational changes. *J. Chem. Phys.* 79:2042–2053.

Ahmed, A. M., B. F. Campbell, D. Caruso, M. R. Chance, M. D. Chavez, S. H. Courtney, J. M. Friedman, I. E. T. Iben, M. R. Ondrias, and M. Yang. 1991. Evidence for proximal control of ligand specificity in heme proteins: absorption and Raman studies of cryogenically trapped photoproducts of ligand bound myoglobins. *Chem. Phys.* 158:329–351.

Ansari, A., J. Berendzen, D. Braunstein, B. R. Cowen, H. Frauenfelder, M. K. Hong, I. E. T. Iben, J. B. Johnson, P. Ormos, T. B. Sauke, R. Scholl, A. Schulte, P. J. Steinbach, J. Vittitow, and R. D. Young. 1987. Rebinding and relaxation in the myoglobin pocket. *Biophys. Chem.* 26:337–355.

Austin, R. H., K. W. Beeson, L. Eisenstein, H. Frauenfelder, and I. C. Gunsalus. 1975. Dynamics of ligand binding to myoglobin. *Biochemistry.* 14:5355–5373.

Bangcharoenpaurpong, O., K. T. Schomaker, and P. M. Champion. 1984. A resonance Raman investigation of myoglobin and hemoglobin. *J. Am. Chem. Soc.* 106:5688–5698.

Bevington, P. R. 1969. Data Reduction and Error Analysis for the Physical Sciences. McGraw-Hill, New York.

Boffi, A., D. Verzilli, E. Chiancone, M. Leone, A. Cupane, V. Militello, E. Vitrano, L. Cordone, W. Yu, and E. E. Di Iorio. 1994. Stereodynamic properties of the cooperative homodimeric *Scapharca inaequivalvis* hemoglobin studied through optical absorption spectroscopy and ligand rebinding kinetics. *Biophys. J.* 67:1713–1723.

Bosenbeck, M., R. Schweitzer-Stenner, and W. Dreybrodt. 1992. pH-induced conformational changes of the Fe^{2+}-N_ε(His F8) linkage in deoxyhemoglobin trout IV detected by the Raman active Fe^{2+}-N_ε(His F8) stretching mode. *Biophys. J.* 61:31–41.

Buhks, E., and J. Jortner. 1985. The dynamics of carbon monoxide binding to hemoglobin and to cytochrome. *J. Chem. Phys.* 83:4456–4462.

Champion, P. M. 1992. Raman and kinetic studies of myoglobin structure and dynamics. *J. Raman Spectrosc.* 23:557–567.

Chaudhury, N. K., G. S. S. Saini, and L. Verma. 1992. Stereochemical aspects of axial ligation in ferrous iron-porphyrins probed by resonance Raman spectroscopy. *Spectrochim. Acta.* 48A:1589–1599.

Christian, J. F., M. Unno, J. T. Sage, P. M. Champion, E. Chien, and S. G. Sligar. 1997. Spectroscopic effects of polarity and hydration in the distal heme pocket of deoxymyoglobin. *Biochemistry.* 36:11198–11204.

Chu, K., R. M. Ernst, H. Frauenfelder, J. R. Mourant, G. U. Nienhaus, and R. Philipp. 1995. Light-induced and thermal relaxation in a protein. *Phys. Rev. Lett.* 74:2607–2610.

Cordone, L., A. Cupane, M. Leone, and E. Vitrano. 1986. Optical absorption spectra of deoxy- and oxyhemoglobin in the temperature range 300–20 K. Relation with protein dynamics. *Biophys. Chem.* 24: 259–275.

Cordone, L., A. Cupane, M. Leone, and E. Vitrano. 1988. Interaction between external medium and haem pocket in myoglobin probed by low-temperature optical spectroscopy. *J. Mol. Biol.* 199:213–218.

Cupane, A., M. Leone, and E. Vitrano. 1993. Protein dynamics: conformational disorder, vibrational coupling and anharmonicity in deoxyhemoglobin and myoglobin. *Eur. Biophys. J.* 21:385–391.

Cupane, A., M. Leone, E. Vitrano, L. Cordone, U. R. Hiltpold, K. H. Winterhalter, W. Yu, and E. E. Di Iorio. 1993. Structure-dynamics function relationships in Asian elephant (*Elephas maximus*) myoglobin. An optical spectroscopy and flash photolysis study on functionally important motions. *Biophys. J.* 65:2461–2472.

Cusack, S., and W. Doster. 1990. Temperature dependence of the low-frequency dynamics of myoglobin. Measurement of the vibrational frequency distribution by inelastic neutron scattering. *Biophys. J.* 58: 243–251.

Demmel, F., W. Doster, W. Petry, and A. Schulte. 1997. Vibrational frequency shifts as a probe of hydrogen bonds: thermal expansion and glass transition of myoglobin in mixed solvents. *Eur. Biophys. J.* 26: 327–335.

Diehl, M., W. Doster, W. Petry, and H. Schober. 1997. Water-coupled low-frequency modes of myoglobin and lysozyme observed by inelastic neutron scattering. *Biophys. J.* 73:2726–2732.

Di Iorio, E. E., U. R. Hiltpold, D. Filipovic, H. Winterhalter, E. Gratton, E. Vitrano, A. Cupane, M. Leone, and L. Cordone. 1991. Protein dynamics. Comparative investigation on heme-proteins with different physiological roles. *Biophys. J.* 59:742–754.

Di Pace, A., A. Cupane, M. Leone, E. Vitrano, and L. Cordone. 1992. Protein dynamics. Vibrational coupling, spectral broadening mechanisms, and anharmonicity effects in carbonmonoxy heme proteins studied by the temperature dependence of the Soret band lineshape. *Biophys. J.* 63:475–484.

Doster, W., S. Cusack, and W. Petry. 1989. Dynamical transition of myoglobin revealed by inelastic neutron scattering. *Nature.* 337: 754–756.

Dvivedi, A., T. Pederson, and P. G. Debrunner. 1979. Recoilless fraction of iron proteins in frozen solution. *J. Physique C2.* 40:C2–531–C2–533.

Egeberg, K. D., B. A. Springer, S. A. Martinis, S. G. Sligar, D. Morikis, and P. M. Champion. 1990. Alteration of sperm whale myoglobin heme axial ligation by site-directed mutagenesis. *Biochemistry.* 29: 9783–9791.

Frauenfelder, H., N. A. Alberding, A. Ansari, D. Braunstein, B. R. Cowen, M. K. Hong, I. E. T. Iben, J. B. Johnson, S. Luck, M. C. Marden, J. R. Mourant, P. Ormos, L. Reinisch, R. Scholl, A. Schulte, E. Shyamsunder, L. B. Sorensen, P. J. Steinbach, A. Xie, R. D. Young, and K. T. Yue. 1990. Proteins and pressure. *J. Phys. Chem.* 94:1024–1037.

Frauenfelder, H., F. Parak, and R. D. Young. 1988. Conformational substates in proteins. *Annu. Rev. Biophys. Biochem.* 17:451–479.

Frauenfelder, H., G. A. Petsko, and D. Tsernoglu. 1979. Temperature-dependent x-ray diffraction as a probe of protein structural dynamics. *Nature.* 280:558–563.

Galkin, O., S. Buchter, A. Tabirian, and A. Schulte. 1997. Pressure effects on the proximal heme pocket in myoglobin probed by Raman and near-infrared absorption spectroscopy. *Biophys. J.* 73:2752–2763.

Gelin, B. R., A. W.-M. Lee, and M. Karplus. 1983. Hemoglobin tertiary structural change on ligand binding. Its role in the co-operative mechanism. *J. Mol. Biol.* 171:489–559.

Gilch, H., W. Dreybrodt, and R. Schweitzer-Stenner. 1995. Thermal fluctuation between conformational substates of the Fe^{2+}-$N_\varepsilon(His^{F8})$ linkage in deoxymyoglobin probed by the Raman-active Fe-$N_\varepsilon(His^{F8})$ stretching vibration. *Biophys. J.* 69:214–227.

Gilch, H., R. Schweitzer-Stenner, and W. Dreybrodt. 1993. Structural heterogeneity of the Fe^{2+}-$N_\varepsilon(His^{F8})$ bond in various hemoglobin and myoglobin derivatives probed by the Raman-active iron histidine stretching mode. *Biophys. J.* 65:1470–1485.

Gilch, H., R. Schweitzer-Stenner, W. Dreybrodt, M. Leone, A. Cupane, and L. Cordone. 1996. Conformational substates of the Fe^{2+}-$N_\varepsilon(His^{F8})$ linkage in deoxymyoglobin and hemoglobin probed in parallel by the Raman band of the Fe-His stretching vibration and the near-infrared absorption band III. *Int. J. Quant. Chem.* 59:301–313.

Hartmann, H., F. Parak, W. Stegemann, G. A. Petsko, D. Ringe Ponzi, and H. Frauenfelder. 1982. Conformational substates in a protein: structure and dynamics of metmyoglobin at 80 K. *Proc. Natl. Acad. Sci. USA.* 79:4967–4971.

Hartmann, H., S. Zinser, P. Komminos, G. U. Nienhaus, and F. Parak. 1996. X-ray structure determination of a metastable state of carbonmonoxy myoglobin after photodissociation. *Proc. Natl. Acad. Sci. USA.* 93:7013–7016.

Henry, E. R., W. A. Eaton, and R. M. Hochstrasser. 1986. Molecular dynamics simulations of cooling in laser-excited heme proteins. *Proc. Natl. Acad. Sci. USA.* 83:8982–8986.

Hirota, S., T. Li, G. N. Phillips, Jr., J. S. Olson, M. Mukai, and T. Kitagawa. 1996. Perturbations of the Fe-O_2 bond by nearby residues in heme pocket: observation of the $\nu_{Fe—O_2}$ Raman bands for oxymyoglobin mutants. *J. Am. Chem. Soc.* 118:7845–7846.

Hori, H., and T. Kitagawa. 1980. Iron-ligand stretching band in the resonance Raman spectra of ferrous iron porphyrin derivatives. Importance as a probe band for quarternary structure of hemoglobin. *J. Am. Chem. Soc.* 102:3608–3613.

Jortner, J., and J. Ulstrup. 1979. Dynamics of nonadiabatic atom transfer in biological systems. Carbon monoxide binding to hemoglobin. *J. Am. Chem. Soc.* 101:3744–3754.

Keller, H., and P. G. Debrunner. 1980. Evidence for conformational and diffusional mean square displacements in frozen aqueous solution of oxymyoglobin. *Phys. Rev. Lett.* 45:68–71.

Kitagawa, T. 1988. The heme protein structure and the iron histidine stretching mode. *In* Biological Application of Raman Spectroscopy, Vol. III. T. G. Spiro, editor. Wiley and Sons, New York. 97–131.

Koningstein, J. A. 1972. Introduction to the Theory of the Raman Effect. D. Riedel, Dordrecht, the Netherlands.

La Mar, G. N., D. L. Budd, and H. Goff. 1977. Assignment of proximal histidine proton NMR peaks in myoglobin and hemoglobin. *Biochem. Biophys. Res. Commun.* 77:104–110.

Lax, M. 1952. The Franck-Condon principle and its application to crystals. *J. Chem. Phys.* 20:1752–1760.

Li, X.-Y., and Z. Zgierski. 1992. Iron motion in a five-coordinated heme model. *Chem. Phys. Lett.* 188:16–20.

Liddington, R., Z. Derewenda, G. Dodson, and D. Harris. 1988. Structure of the liganded T state of haemoglobin identifies the origin of cooperative oxygen binding. *Nature.* 331:725–728.

Lingle, R., Jr., X. Xu, H. Zhu, S.-C. Yu, and J. B. Hopkins. 1991. Picosecond Raman study of energy flow in a photoexcited heme protein. *J. Phys. Chem.* 95:9320–9331.

Markham, J. J. 1959. Interaction of normal modes with electron traps. *Rev. Mod. Phys.* 31:956–989.

Marks, S., P. A. Cornelius, and C. B. Harris. 1980. A critical test of vibrational dephasing theories in solids using spontaneous Raman scattering in isotropically mixed crystals. *J. Chem. Phys.* 73:3069–3081.

Mayo, K. H., D. Kucheida, F. Parak, and J. C. W. Chien. 1983. Structural dynamics of human deoxyhemoglobin and hemochrome investigated by nuclear gamma resonance absorption (Mössbauer) spectroscopy. *Proc. Natl. Acad. Sci. USA.* 80:5294–5296.

Melchers, B., E. W. Knapp, F. Parak, L. Cordone, A. Cupane, and M. Leone. 1995. Structural fluctuations of myoglobin derived from normal mode analysis: comparison with Mössbauer, resonance Raman, and absorption spectroscopy. *Biophys. J.* 70:2092–2099.

Nagai, K., and T. Kitagawa. 1980. Differences in Fe(II)-N_ε(His-F8) stretching frequencies between deoxyhemoglobins in the two alternative quarternary structures. *Proc. Natl. Acad. Sci. USA.* 77:2033–2037.

Nagai, K., G. N. La Mar, T. Jue, and H. F. Bunn. 1982. Proton magnetic resonance investigation of the influence of quarternary structure on iron-histidine bonding in deoxyhemoglobins. *Biochemistry.* 21: 842–847.

Nienhaus, G. U., H. Frauenfelder, and F. Parak. 1992a. Structural fluctuations in glass-forming liquids: Mössbauer spectroscopy on iron in glycerol. *Phys. Rev.* B3:3345–3350.

Nienhaus, G. U., J. R. Mourant, K. Chu, and H. Frauenfelder. 1994. Ligand binding to heme proteins: the effect of light on ligand binding in myoglobin. *Biochemistry.* 33:13413–13430.

Nienhaus, G. U., J. R. Mourant, and H. Frauenfelder. 1992b. Spectroscopic evidence for conformational relaxation in myoglobin. *Proc. Natl. Acad. Sci. USA.* 89:2902–2906.

Ondrias, M. R., D. L. Rousseau, and S. R. Simon. 1981. Structural changes at the heme induced by freezing hemoglobin. *Science.* 213:657–659.

Ondrias, M. R., D. L. Rousseau, T. Kitagawa, M. Ikeda-Saito, T. Inubushi, and T. Yonetani. 1982a. Quaternary structure changes in iron-cobalt hybrid hemoglobins detected by resonance Raman scattering. *J. Biol. Chem.* 257:8766–8770.

Ondrias, M. R., D. L. Rousseau, and S. R. Simon. 1982b. Resonance Raman detection of structural dynamics at the active site in hemoglobin. *Proc. Natl. Acad. Sci. USA.* 79:1551–1554.

Ondrias, M. R., D. L. Rousseau, and S. R. Simon. 1983. Resonance Raman spectra of photodissociated carbonmonoxy hemoglobin and deoxy hemoglobin at 10 K. *J. Biol. Chem.* 258:5638–5642.

Parak, F., and E. W. Knapp. 1984. A consistent picture of protein dynamics. *Proc. Natl. Acad. Sci. USA.* 81:7088–7092.

Parak, F., E. W. Knapp, and D. Kucheida. 1982. Protein dynamics. Mössbauer spectroscopy on deoxymyoglobin crystals. *J. Mol. Biol.* 161: 177–194.

Perutz, M. F. 1989. Mechanisms of cooperativity and allosteric regulation in proteins. *Q. Rev. Biophys.* 22:139–236.

Petrich, J. W., J. L. Martin, D. Houde, C. Poyart, and A. Orszag. 1987. Time-resolved Raman spectroscopy with subpicosecond resolution: vibrational cooling and delocalization of strain energy in photodissociated (carbonmonoxy)hemoglobin. *Biochemistry.* 26:7914–7923.

Post, F., W. Doster, G. Karvounis, and M. Settles. 1993. Structural relaxation and nonexponential kinetics of CO-binding to horse myoglobin: multiple flash photolysis experiments. *Biophys. J.* 64:1833–1842.

Powers, L., B. Chance, M. Chance, B. Campbell, J. Friedman, S. Khalid, C. Kumar, A. Naqui, K. S. Reddy, and Y. Zhou. 1987. Kinetic, structural, and spectroscopic identification of geminate states of myoglobin: a ligand binding site on the reaction pathway. *Biochemistry.* 26: 4785–4796.

Rosenfeld, Yu. B., and S. S. Stavrov. 1994. Anharmonic coupling of soft modes and its influence on the shape of the iron-histidine resonance Raman band of heme proteins. *Chem. Phys. Lett.* 229:457–464.

Rousseau, D. L., and P. V. Argade. 1986. Metastable photoproducts from carbon monoxide myoglobin. *Proc. Natl. Acad. Sci. USA.* 83: 1310–1314.

Rousseau, D. L., and J. M. Friedman. 1988. Transient and cryogenic studies of photodissociated hemoglobin and myoglobin. *In* Biological Application of Raman Spectroscopy, Vol. III. T. G. Spiro, editor. Wiley and Sons, New York. 133–215.

Sage, J. T., K. T. Schomacker, and P. M. Champion. 1995. Solvent-dependent structure and dynamics in myoglobin. *J. Phys. Chem.* 99: 3394–3405.

Sassaroli, M., S. Dasgupta, and D. L. Rousseau. 1986. Cryogenic stabilization of myoglobin photoproducts. *J. Biol. Chem.* 261:13704–13713.

Schlichting, I., J. Berendzen, G. N. Phillips, Jr., and R. M. Sweet. 1994. Crystal structure of an intermediate of CO binding to myoglobin. *Nature.* 371:808–812.

Settles, M., and W. Doster. 1996. Anomalous diffusion of adsorbed water: a neutron scattering study of hydrated myoglobin. *Faraday Discuss.* 103:269–279.

Shelby, R. M., C. B. Harris, and P. A. Cornelius. 1979. The origin of vibrational dephasing of polyatomic molecules in condensed phases. *J. Chem. Phys.* 70:34–41.

Simpson, M. C., E. S. Peterson, C. F. Shannon, D. D. Eads, J. M. Friedman, C. M. Cheatum, and M. R. Ondrias. 1997. Transient Raman observations of heme electronic and vibrational photodynamics in deoxyhemoglobin. *J. Am. Chem. Soc.* 119:5110–5117.

Spiro, T. G. 1988. Resonance Raman spectroscopy of metalloporphyrins. *In* Biological Application of Raman Spectroscopy, Vol. III. T. G. Spiro, editor. Wiley and Sons, New York. 1–37.

Šrajer, V., and P. M. Champion. 1991. Investigations of optical line shapes and kinetic hole-burning in myoglobin. *Biochemistry.* 30:7390–7402.

Šrajer, V., L. Reinisch, and P. M. Champion. 1988. Protein fluctuations, distributed coupling, and the binding of ligands to heme proteins. *J. Am. Chem. Soc.* 110:6656–6670.

Stavrov, S. S. 1993. The effect of iron displacement out of the porphyrin plane on the resonance Raman spectra of heme proteins and iron porphyrins. *Biophys. J.* 65:1942–1950.

Stavrov, S. S., and B. Kushkuley. 1993. *In* Fifth International Conference on the Spectroscopy of Biological Molecules. Th. Theophanides, J. Anastassopoulou, and N. Fotopoulos, editors. Kluwer Academic Publishers, Dordrecht, the Netherlands. 305–306.

Steinbach, P. J., A. Ansari, J. Berendzen, D. Braunstein, K. Chu, B. R. Cowen, D. Ehrenstein, H. Frauenfelder, J. B. J. Johnson, D. C. Lamb, C. Luck, J. R. Mourant, G. U. Nienhaus, P. Ormos, R. Philipp, A. Xie, and R. D. Young. 1991. Ligand binding to heme proteins: connection between dynamics and function. *Biochemistry.* 30:3988–4001.

Teng, T.-Y., V. Šrajer, and K. Moffat. 1994. Photolysis-induced structural changes in single crystals of carbonmonoxy myoglobin at 40 K. *Nature Struct. Biol.* 1:701–705.

Teng, T.-Y., V. Šrajer, and K. Moffat. 1997. Initial trajectory of carbon monoxide after photodissociation from myoglobin at cryogenic temperatures. *Biochemistry.* 36:12087–12100.

Wang, C.-M., and W. S. Brinigar. 1979. A correlation of the visible and Soret spectra of dioxygen- and carbon monoxide-heme complexes and five-coordinate heme complexes with the spectra of oxy-, carboxy-, and deoxyhemoglobin. *Biochemistry.* 22:4960–4977.

Windholz, M., S. Budavari, L. Y. Stroumtsos, and M. N. Fertig. 1976. The Merck Index. An Encyclopedia of Chemicals and Drugs. Merck and Co., Rahway, NJ.

Zhu, L., J. T. Sage, and P. Champion. 1993. Quantitative structural comparisons of heme protein crystals and solutions using resonance Raman spectroscopy. *Biochemistry.* 32:11181–11185.